COUPLING INFECTIOUS DISEASE MODEL AND GIS FOR LIVING MATERIAL SUPPLY ANALYSIS DURING COVID-19 OUTBREAK —— TAKING SHENZHEN AS AN EXAMPLE

XIAO Jie [1,2], ZHAO Tianhong [1,2], GU Yu [1,2], TU Wei [1,2,3*]

1 School of Architecture and Urban Planning, Shenzhen University, Shenzhen 518060, China
xiaojie2021@email.szu.edu.cn;zhaotianhong2016@email.szu.edu.cn;guyuleaves@163.com;tuwei@szu.edu.cn
2 Guangdong Key Laboratory of Urban Informatics, Shenzhen Key Laboratory of Spatial Smart Sensing and Service, Shenzhen 518060, China
3 Key Laboratory for Geo-Environmental Monitoring of Great Bay Area, MNR, Shenzhen 518060, China

Commission IV, WG IV/3

KEY WORDS: Infectious disease simulation, GIS, spatial analysis, material guarantee, supply and demand

ABSTRACT:

The COVID-19 epidemic has posed a grave threat to human life. The stay-at-home quarantine is an effective method of minimizing physical contact and the risk of COVID-19 transmission. However, the supply of living materials (such as meat, vegetables, grain, and oil) has become a great challenge as residents' activities have been restricted. In this paper, we present a spatial analysis framework for the supply of living materials during COVID-19 outbreak by coupling an infectious disease model with geographic information system (GIS). First, a virus spreading spatial simulation model is developed by combining cellular automata (CA) and Susceptible-Exposed-Infected-Recovered-Death (SEIRD) to estimate COVID-19's spreading under various scenarios. Second, the demand and supply of living materials in the impacted residents are calculated. Finally, the imbalance of the supply and demand of the living materials is assessed. We conduct experiments in Shenzhen. The experimental results show that localities with supply-demand mismatches are primarily concentrated in the southwest of Bao'an District, the southern of Longhua District, and Longgang District. Additionally, the spatial distribution of the mismatch level between supply and demand for living materials in Shenzhen exhibits a significant agglomeration effect, manifested as "low-low" and "high-high" agglomeration. The spatial agglomeration effect of material mismatch has increased with the spread of the epidemic. These results support the prevention and control of the COVID-19 spreading.

1. INTRODUCTION

Since the outbreak of the COVID-19, it has caused serious disasters to the worldwide health and economy. According to World Health Organization (WHO) statistics, the number of deaths caused by COVID-19 is 1.9 million in 2020 and 3.5 million in 2021. At present, the COVID-19 epidemic is still raging around the world. Epidemic prevention and control remains the top priority. Keeping a healthy social distance is the key to epidemic prevention and control (Ma et al., 2020), which can effectively prevent the spread of the virus. But a series of epidemic control measures such as stay-at-home and the limitation of small supermarkets will affect the supply of people's living materials (such as meat, vegetables, grain, and oil) and bring great inconvenience to our life. The provision of basic living material is critical for inhabitants' survival during the COVID-19 outbreak. For example, previous study has shown that strict social distancing is the key to reducing the number of infections in Wuhan and Hubei (Firozjaei et al., 2021). After the outbreak of the epidemic, relevant departments organized emergency supply guarantees based on ultra-normal demand, coordinating the resources of all parties to increase the supply of living materials.

It is necessary to forecast the future epidemic condition in advance and then adopt effective controlling measures for living material supply. In 1927, Kermack et al., (1927) established the classic Susceptible-Infected-Recovered (SIR) infectious disease model, they divided the research subjects into several different groups, including susceptible, infected and cured. The series of previous basic studies laid the foundation for the subsequent development of infectious disease models, and then many scholars began to enrich and propose new infectious disease models, i.e., the Susceptible-Exposed-Infected-Recovered (SEIR) model, etc (Lahrouz et al., 2013). With the development of computing technology, the simulation model based on cellular automata (CA) is possible. Among various mathematical methods for describing the spread of infectious diseases, CA makes it possible to explicitly simulate both the spatial and temporal evolution of epidemics with intuitive local rules. In the field of infectious disease research, the combination of CA and classical infectious disease models has become a new research direction in the field of infectious diseases (White et al., 2007).

During the global fight against the COVID-19 epidemic, scholars have also conducted extensive researches on epidemic spread and trend prediction using infectious disease models. In 2021, Alaˈraj et al.(2021) used public data to study the properties associated with the COVID-19 pandemic to develop a dynamic hybrid model based on Susceptible-Exposed- Infected-Recovered-Death(SEIRD) and ascertainment rate with automatically selected parameters. Götz et al.(2020) presented

* Corresponding author

an extended SEIRD model to describe the disease dynamics in Germany. Annas et al.(2020) constructed the SEIR model for COVID-19, and their simulation results showed that the vaccine can accelerate COVID-19 healing and maximum isolation can slow the spread of COVID-19. Yang et al.(2020) used the SEIR model to predict that the domestic epidemic will peak in late February, 2020. By combining CA and classical differential equations, Schimit et al.(2021) described a SEIR model integrating the probabilistic CA and ordinary differential equations for the transmission of COVID-19. Cavalcante et al.(2021) applied the obtained parameters to the CA model. These studies are proved to represent an essential tool in predicting the spread of the virus in confined spaces with random movements of people.

The spread of the epidemic affects people's living. From the spatial perspective, Geographic Information System (GIS) can be used to study the supply of urban public services such as living materials supply. Charreire et al. (2010) reviewed the literature and summarized two different spatial methods for detecting people's material security using GIS. Density method used the buffer function or spatial clustering to quantify food store availability. Whereas the proximity method assesses the distance to a food store by measuring distance or travel time. LeClair et al. (2014) examined the food availability in Bridgeport, Connecticut by using GIS mapping and field observations. The results showed that the resulting maps output from GIS can mine general food accessibility issues. Apparicio et al., (2007) presented the hierarchical cluster analysis to identify food supply and demand in Montreal. Three methods measuring supermarket accessibility are used, including the proximity, the diversity and the volatility in food and price. The spatial analysis method can effectively capture the geographical isolation between the supply side and the demand side (Zhao et al., 2021). These studies demonstrate the ability of spatial analysis rooted in GIS for the mismatch of the demand and the supply.

However, under the epidemic situation, the management and control policies of the residential area will greatly affect the residents to obtain the living materials, i.e., meat, rice, water, etc. With the development the COVID-19, more and more people may be infected. The area affected by the the controlling and prevention measures may be large, the associated living materials would increase. Therefore, it is necessary to investigate the mismatch between the demand and the supply of the COVID-19. Coupling the CA-based spatial simulation for the COVID-19, this paper employs spatial analysis to assess the mismatch of living material supply and demand., The results will benefit the controlling and prevention of COVID-19.

The remainder of this paper is as following: Section 2 introduces the presented method. Section 3 describe the study area and data. Section 4 reports the results and analysis the mismatch of the living material demand and supply in multiple scenarios. Section 5 concludes this research and outlook future work.

2. METHODOLOGY

2.1 Overall Framework

This study presents the spatial analysis framework for evaluating the mismatch of the living material demand and supply for the controlling and prevention of the COVID-19. Figure 1 shows the workflow of the presented framework. First, the COVID-19 epidemic situation is spatially simulated using the CA-based SEIRD model. Spatial distribution of the infected cases will be obtained. Then, the demand of living materials are estimated by using the residential building data. At the same time, the supply degree are calculated through service area analysis using the data including supermarkets and road networks. Thus, the gap between the demand and the supply could be detected. Then, the mismatch level of the demand and the supply in the city will be spatially analyzed.

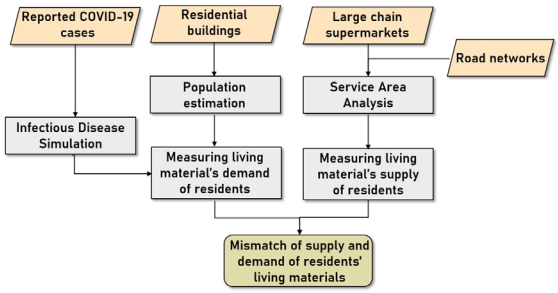

Figure 1. The workflow of the presented framework

2.2 Spatial simulation of the COVID-19 spreading

2.2.1 The basic SEIRD model

The SEIRD model can clearly describe the logical relationship of virus transmission and can predict the trend of the outbreak more accurately. Figure 2 shows the virus infection process. It divides the total population into susceptible persons S (Susceptible), latent persons E (Exposed), infected persons I (Infected), cured persons R (Recovered) and dead persons D (Death).

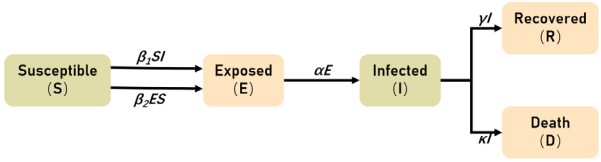

Figure 2. SEIRD model propagation mechanism

$S(t)$, $E(t)$, $I(t)$, $R(t)$, $D(t)$ respectively represent the number of susceptible, latent, infected, cured, and dead persons at time t. The total number of people in the model is N, then:

$$S(t) + E(t) + I(t) + R(t) + D(t) = N \quad (1)$$

Symbol	Annotation
N	total number of people
$\beta_1 = c\rho_1$	transmission rate of infected persons
$\beta_2 = c\rho_2$	latent transmission rate
c	contact rate
ρ_1	infection probability of the person contacting the infected cases
ρ_2	probability of contact with the latent person being infected
$1/\alpha$	incubation period
$1/\gamma$	rehabilitation period
κ	mortality

Table 1. The mathematic symbols and the annotations in SEIRD model

The SEIRD model makes the following assumptions:
(1) The number of total populations is constant. The model does not consider the possible population change such as migration, birth, death, and so on.
(2) The model does not consider demographic elements, that is, the birth rate and death rate of the population do not exist in the model;
(3) The population contacts in the model is all complete contacts.

Based on the virus spreading mechanism in Figure 2, the SEIRD model is constructed with following differential equation:

$$\begin{cases} \frac{dS}{dt} = \frac{\beta_1 SI}{N} - \frac{\beta_2 ES}{N} \\ \frac{dE}{dt} = \frac{\beta_1 SI}{N} - \frac{\beta_2 ES}{N} - \alpha E \\ \frac{dI}{dt} = \alpha E - \gamma I - \kappa I \\ \frac{dR}{dt} = \gamma I \\ \frac{dy}{dx} = \kappa I \end{cases} \quad (2)$$

2.2.2 CA-based SEIRD model

Traditional differential equation based SEIRD models have several limitations: they are dependent on initial values; they do not have subjective dynamics to describe complex stochastic behaviors. The integration of CA and differential equation-based SEIRD model can describe the complex stochastic behaviors of various populations and display the epidemic transmission at different time steps.

CA simulates the future spatial conditions according to the conditions and the evolution rules Specifically, the basic unit named cell will convert from its current state to another state according to the neighbourhood conversion rules. We use the Moore-type cell neighbors with a radius of 1, as figure 3 shows. In the SEIRD model, β_1 and β_2 represent the transmission rate of infected and latent persons; therefore, they are as the neighbourhood conversion rules in CA. For example, the susceptible cell will convert to latent state with the probability of β_1 when it contacts the infected cells. Similarly, the susceptible cell will convert to latent with the probability of β_2 when it contacts the latent cells. In addition, α represents the ratio of latent persons to infected, it means the latent cell will convert to infected at the ratio of α. Besides,γrepresents the probability of the infected person recovering, and the infected cell will convert to cured with the probability of γ. Finally, κ represents the death rate of the infected person, and the infected cell will convert to dead with the probability of κ.

In summary, the following CA model is constructed for the SEIRD:
1. Cell
A cell is the basic unit of a CA model and is distributed over the study area.
2.Cell space
The simulation space is two-dimensional, which is comprised of totally $n * m,$ cells.
3. Cell state
S_{ij}^t indicates the state of the cells l with coordinates(i, j) at time t. The cell space state can be expressed as:

$$S(t) = \{S_{11}^t, S_{12}^t, \dots, S_{21}^t, S_{22}^t, \dots, S_{ij}^t\} i, j \in n \quad (3)$$

Each cell in the model has five possible cellular states:

$$S_{ij}^t = \{0,1,2,3,4\}\, i, j \in n \quad (4)$$

Among them, 0 represents that the cell is in the susceptible state, while the 1, 2, 3, and 4 respectively represent the latent, infected, cured, and dead state.

While the initial state of a traditional CA model is given randomly, in this study, the spatial distribution of the reported COVID-19 cases can be used as the initial state.

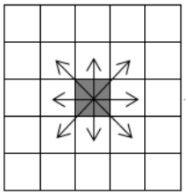

Figure 3. Moore-type cell neighbors

4. Neighbourhood conversion rules
CA adopts periodic boundary conditions. In the initial state, all cells' state is set as $S_{ij}^t = 0$ Then, the cells which are infected are set as $S_{ij}^t = 2$ From time $t = 0$, all cells update their state according to the following neighbourhood conversion rules with a discrete time step until simulation ends:

① When $S_{ij}^t = 0$, the cell in (i, j) is susceptible, and calculate its adjacency matrix H according to its neighborhood cells:

$$H = \begin{bmatrix} S_{i-1,j-1}^t & S_{i-1,j}^t & S_{i-1,j+1}^t \\ S_{i,j-1}^t & S_{i,j}^t & S_{i,j+1}^t \\ S_{i+1,j-1}^t & S_{i+1,j}^t & S_{i+1,j+1}^t \end{bmatrix} \quad (5)$$

Therefore, the number of neighborhood cells with state S of 1 and 2 is counted respectively, and the former represents the number of latent people using $M_{ij}(t)$ to indicate and the latter means the number of infected people representing by $\mathrm{N_{ij}(t)}$. If there are multiple infected or latent persons in the neighborhood, P_{ij} indicates whether the cell (i, j) is infected:

$$P_{ij} = 1 - (1 - \beta_1)^{M_{ij}(t)}(1 - \beta_2)^{N_{ij}(t)} \quad (6)$$

If there are infected people in the neighborhood cells, the infected probability of the cell is β_1. If there are lurks in the neighborhood, the corresponding probability is β_2. As known from formula (6), the infection probability of cells is directly proportional to the number of infected and latent persons in their neighbors. If infected, it becomes latent and its cellular state at next time $t + 1$ is $S_{ij}^{t+1} = 1$.

② When $S_{ij}^t = 1$, the cell is latent and remains with the infectious risk. As table 1 shows, $1/\alpha$ indictaes it is in the incubation period. If $t_e < 1/\alpha$, it is still in incubation period; if $t_e > 1/\alpha$, cells become infected. The rules are as follows:

$$\mathrm{S_{ij}^{t+1}} = \begin{cases} 1, & \mathrm{t_e} < \frac{1}{\alpha} \\ 2, & \mathrm{t_e} > \frac{1}{\alpha} \end{cases} \quad (7)$$

③ When $S_{ij}^t = 2$, the cell is infected. According to table 1, $1/\gamma$ represents the rehabilitation period. If $t_i < 1/\gamma$, The cells are still with the infection state; if $t_i > 1/\gamma$, the cell has exceeded the recovery period, and it is converted to the dead with the probability of κ. The remaining cells become cured and gain permanent immune ability, and no longer participate in the transmission process. The rules are as follows:

$$S_{ij}^{t+1} = \begin{cases} 2, & t_i < \frac{1}{\gamma} \\ 3, & t_i > \frac{1}{\gamma} \text{ and be cured} \\ 4, & t_i > \frac{1}{\gamma} \text{ and die} \end{cases} \quad (8)$$

④ When $S_{ij}^t = 3$, the cells are cured. They have obtained permanent immunity and will not be infected again. The cellular state remained $S_{ij}^{t+1} = 3$ until simulation ends.

⑤ When $S_{ij}^t = 4$, the cell is dead. The cell state remains $S_{ij}^t = 4$ until simulation ends.

Besides the Neighbourhood conversion rules, the mobility description in CA is also an important factor for the simulation. Without considering the external intervention measures, the residents should move randomly within the neighborhoods. Therefore, the model adopts the random moving operation.

5.Time
The model takes the day as the basic temporal unit, that is, one day is the minimum temporal interval for the epidemic spread and evolution. In addition, the holding time of each cell state should be counted, and the cell latency time is recorded as t_e. The time of cellular infection was recorded as t_i.

2.3 Analysis on supply and demand of residents' living materials

2.3.1 Demand degree of residents' living materials

With CA, we can get the spatial spread of the virus in multiple scenarios as the COVID-19 would infect many people. The demand for living materials in these restricted buildings mainly depends on its resident population. In this study, the population is estimated according to the building data and the total population. The calculation formula is:

$$P_i' = \frac{S_i L_i}{\sum_{n=1}^{m} S_n L_n} * P_T \quad (9)$$

Where P_i' = the estimated population of the building i
S_i = the floor area of the building i
L_i = the floor of the building i
m = the total number of buildings
P_T = the total population of study area

For the cell, we estimate its population as below:

$$p_j = \sum_{i=1}^{h} P_i' \quad (10)$$

Where p_j = the estimated population of the cell j
h = the total number of buildings belonging to the cell j

We calculate the total living material demand with the estimated population. Generally, an adult need vegetable, fruit, meat, cereals, oils, eggs, and other daily necessities. Table 2 shows the quantity of basic living materials. Hence, the total demand of the cell can be estimated as Eq (11):

Type	Quantity (g)
vegetable and fruit	600
meat	125
Cereals and oils	340
Eggs	37.5
Daily Necessities	250

Table 2. Average daily living needs of an adult

$$D_j = p_j * K \quad (11)$$

Where D_j = the material demand of the cell j
K = the total daily living needs of an adult

2.3.2 Supply degree of residents' living materials

The living materials will be transported from supermarkets to the residential buildings. We assume that large supermarkets are considered as the supply source of living materials. Here, we classify the supply level of the supermarket to the surrounding areas based on the walking time to the supermarket.

Walking time from supermarket (t)	Supply level	Weight (ε)
t<5 min	Strong (ⅰ)	0.4
5 min<t<10 min	Slightly strong (ⅱ)	0.3
10 min<t<20 min	Slightly weak (ⅲ)	0.2
20 min<t<30 min	Weak (ⅳ)	0.1

Table 3. Classification of supermarket supply level to surrounding areas

The supply degree of each cell is calculated according to its covered times by all supermarkets with different supply levels:

$$S_j = \varepsilon_{\text{I}} * \text{Times}_{\text{I}} + \varepsilon_{\text{II}} * \text{Times}_{\text{II}} + \varepsilon_{\text{III}} * \text{Times}_{\text{III}} + \varepsilon_{\text{IV}} * \text{Times}_{\text{IV}} \quad (12)$$

Where S_j = the material supply degree of the cell j
ε_I、ε_{II}、ε_{III}、ε_{IV} = the weights of different grades in Table 3
$Times_I$、$Times_{II}$、$Times_{III}$、$Times_{IV}$ = the number of times that the every building belonging to the cell j is covered by guarantee areas at every levels

2.3.3 Mismatch degree of supply and demand of residents' living materials

When residents inside the building, which impacted by a reported case, are asked to stay at home, people are not free to go out and buy their daily necessities, so they have to rely on government departments to send living materials from nearby large supermarkets to the residential buildings. Thus there may be mismatch between demand and supply, that is, the demand for residents' living materials may not satisfied due to the limited supply ability. This study defines δ to reflect the degree of mismatch between supply and demand:

$$\delta_j = \frac{D_j}{S_j} \quad (13)$$

2.3.4 Spatial distribution pattern of mismatch degree of supply and demand of living materials

In order to reveal the spatial pattern of the mismatch degree of supply and demand of residents' living materials, we use the software Geoda. The spatial weight matrix is constructed with the INVERT_DISTANCE method. Moran's I index is calculated and analyzed in combination with Moran scatter diagram and Lisa agglomeration diagram to detect the spatial agglomeration of the mismatch between supply and demand of living materials.

1) global spatial autocorrelation

Global spatial autocorrelation indicates the overall spatial divergence and aggregation characteristics of the mismatch degree of material supply and demand in the study area. If n represents the total number of samples of a variable and x_i is the observed value of the variable at the location or spatial unit i, the global Moran's I index of the variable is as follows:

$$I = \frac{n\sum_{i=1}^{n}\sum_{j=1}^{n}W_{ij}(x_i-\bar{x})(x_j-\bar{x})}{\sum_{i=1}^{n}\sum_{j=1}^{n}W_{ij}\sum_{i=1}^{n}(x_i-\bar{x})^2}(i \neq j) \quad (14)$$

Where x_i = the observed value of area i
W_{ij} = the spatial weight matrix

The value range of Moran's I index lies in the range [- 1, 1]. A value less than 0 indicates negative correlation, while a value greater than 0 indicates positive correlation, and equal to 0 indicates that each spatial object unit in the study area is independent of each other. The closer the I value is to 1, the more significant the agglomeration effect of an attribute in the spatial distribution of the object is; The closer the I value is to - 1, the more significant the spatial tendency distribution of an attribute of the object is.

2) local spatial autocorrelation

Local spatial autocorrelation reveals the spatial correlation patterns of mismatch degrees of supply and demand of living materials in spatially adjacent regions. The local Moran's I index is used to measure whether there is high or low value local spatial agglomeration in the region. I_i is the local Moran's I index of a region i. The specific formula is as follows:

$$I_i = \frac{(x_i-\bar{x})}{\frac{1}{n}\sum_{i=1}^{n}(x_i-\bar{x})^2}\sum_j W_{ij}(x_i-\bar{x}), i \neq j \quad (15)$$

According to local spatial autocorrelation, the study area can be divided into five types: high-high aggregation, low-low aggregation, low-high aggregation, high-high aggregation and no obvious aggregation.

3. STUDY AREA AND DATA

The research is conducted in Shenzhen, China. Shenzhen is located in the south of China and is a special economic zone, a center of science and technology innovation in China. It has ten administrative districts, with a total area of 1997.47 square kilometers and a population of 17,560,610,000. On January 19, 2020, the first confirmed case of COVID-19 appeared in Shenzhen. On February 7, 2020, Shenzhen Epidemic Prevention and Control Command issued an announcement that residential buildings with confirmed cases were to be placed under hard quarantine for 14 days.

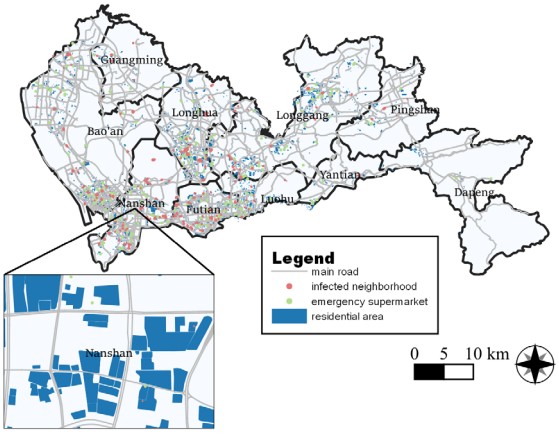

Figure 4. Data used in the study

The research data includes the road network data, COVID-19 case data, large supermarket POI data and residential building data. The road network data comes from OpenStreetMap. The data of COVID-19 cases are from the Shenzhen Municipal Health Commission, and their longitude and latitude are obtained through API from AutoNavi. Large supermarket data is obtained through the API interface provided by AutoNavi. When residents inside the building are asked to segregate at home, large chain supermarkets provide living materials for the buildings. The main supermarkets include the Wal Mart, Vanguard, Renrenle, etc. Residential building data is also obtained through the AutoNav API interface. It possesses various attributes of name, bottom area, floor, etc.

4. RESULTS AND DISCUSSION

To simulate the COVID-19 spreading of different scenarios, the CA-based SEIRD model is implemented. The supply and demand of living materials for residents' daily life under different scenarios is analyzed.

4.1 The COVID-19 spreading simulation results

By fusing the infectious disease models of CA and SEIRD, we simulated the evolution of spatial transmission of COVID-19 at different levels. Figure 5 displays the simulation results. The pink areas indicate these cells will be affected when the proportions of infected areas reach 20%, 40%, 60%, and 80%. Compared with the four results in different infected proportions, it brings out a relatively similar evolutional trend in all regions: By increasing of the infected proportion from 20% to 80%, the affected buildings initially surge and then increase slowly later. Moreover, the main extending and spreading area is in the south of Shenzhen; whereas the unremarkable rise in the residual area. It mainly due to these areas are the most vigorous in Shenzhen, thus they undertake more people flow caused by colossal economical, entertainment and commuting behaviours. The frequent interaction provides suitable curriculum for epidemic virus spread.

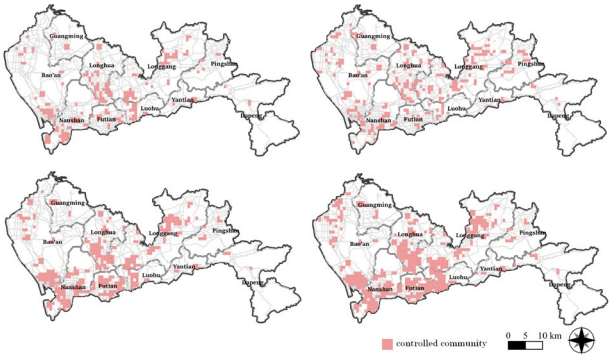

Figure 5. Simulation results of infectious diseases

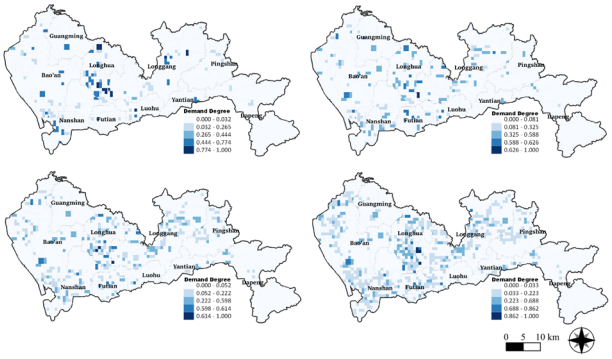

Figure 6. Demand degree of residents' living materials under different extents of simulation

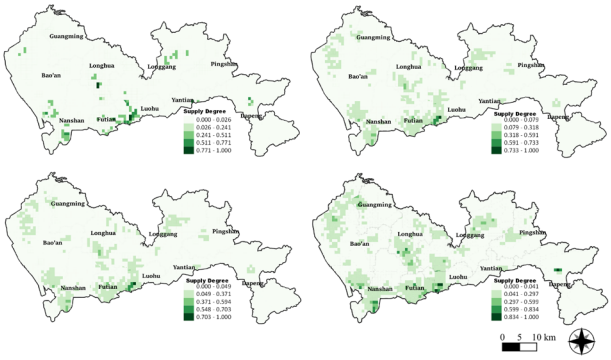

Figure 7. Supply degree of residents' living materials under different extents of simulation

4.2 Supply and demand analysis of living materials

4.2.1 Demand for living materials of residents

With the residential building data, we achieve population estimation and thus calculate the demand for household goods per cell. Figure 6 indicates the changes in the degree of demand for residential living materials under different extents of virus spread simulation. At 20%, the total cell volume is 378 and the total demand is 4916.8 tons, in which the main affected buildings are mostly distributed in the south of Longhua District and the south of Nanshan District. At 40%, the total cell volume is 724 and the total demand is 10229.2 tons. At this stage, with the spread of the virus, the affected buildings are more scattered. At the 60% level, the total cell is 1147, and the total demand is 14750.45 tons, among which the demand for living materials in Futian District and Nanshan District is relatively high, and the frequent movement of population in these two administrative regions leads to a gradual increase in the number of cases in the simulated situation, and more residential buildings are required to be closed, and the demand for living materials from residents who cannot access freely increased. At 80% degree, the total cell amount was 1359 and total demand was 18,964.3 tons. Among the residents requiring home isolation, the demand for residential living materials was higher in the southern of Longhua District, the southern of Nanshan District, Futian District, and the central of Longgang District. In general, with the increase of infected population, the degree of residents' demand for household materials keeps changing spatially. In the early stage of the simulation, the main affected areas were administrative districts with a large population base, such as Longhua District and Longgang District. With the population movement, the virus gradually spreads, at which time cases start to appear in residential buildings in the most frequently populated areas, leading to the need for home isolation in these neighborhoods and a relative increase in their degree of demand for daily living needs.

4.2.2 Supply of living materials for residents

Figure 7 shows the changes in the degree of supply for residential living materials under different extents of virus spread simulation. Under the 20% degree, the number of buildings with restricted access is small at this time, and the stock of large supermarkets can meet the daily needs of these residents. Under the 40% and 60%, the number of cases gradually increases, the number of isolated residential buildings gradually increases, the scope of a certain number of supermarkets that need to supply supplies becomes larger, and the distribution of supermarkets is more sparse in the vicinity of some neighborhoods, such as the southern part of Longhua District and the central part of Longgang District. Under the simulation to 80% degree, almost all large supermarkets provide living materials for the closed residential buildings under the arrangement of government departments, and the degree of supply of living materials for the home isolated citizens in Nanshan District and Longgang District rise.

4.2.3 Mismatch degree of supply and demand of residents' living materials

When there is a confirmed case, the residential building in which it is located will be closed, other residents cannot go out, and their access to household goods is restricted, thus a mismatch between supply and demand for goods may arise. By calculating the demand and supply degrees as described above, we are able to calculate the degree of mismatch between supply and demand. Figure 8 shows the changes in the degree of demand-supply mismatch for residential living materials under different extents of virus spread simulation. At 20% level, the mismatch between supply and demand is mainly distributed in Longhua District, the more notable areas are its north and south, and some scattered places in Longgang District, where the population is more dense, and when there is a case, the relevant residential buildings are closed, and a large number of residents have to stay at home and cannot go out to purchase living supplies. The nearby supermarkets could not supply enough supplies to meet such a large demand. At 40% and 60% levels, the virus gradually spread and an imbalance in the supply and demand of household goods gradually emerged in Bao'an District. Bao'an District is the administrative district with the largest population living in Shenzhen, so in a simulated situation, once a resident is diagnosed, it is extremely easy to spread rapidly through crowd movement. This leads to an aggravation of the epidemic

situation and an increasing number of residential buildings which would be closed. At the simulation to 80% level, mismatch between supply and demand occurs at this time in Yantian District and Dapeng District, where large supermarkets are more sparsely distributed and the accessibility is relatively low, leading to a restricted supply.

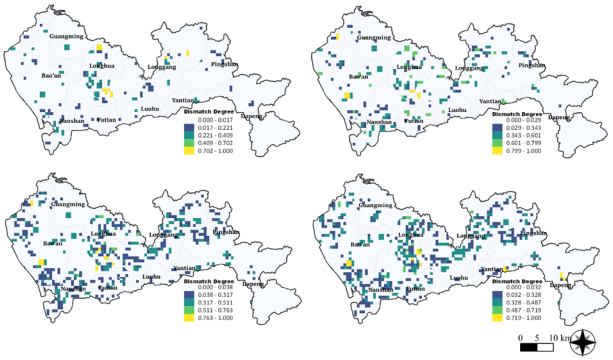

Figure 8. Mismatch degree of supply and demand of residents' living materials under different extents of simulation

No.	Neighborhood's name	District
1	Plum Blossom Villa	Longhua
2	St. Morris	Longhua
3	Taoyuan Residence	Baoan
4	Hongrongyuan One City Center	Longhua
5	Qunle Building	Baoan
6	Telford Garden	Longgang
7	Aegean Sea	Yantian
8	Shapu Second Village	Baoan
9	Lingjian New Village	Dapeng
10	Zhenye City	Longhua

Table 4. The most mismatched 10 neighborhoods

The above table shows the 10 neighborhoods in Shenzhen with the most supply-demand mismatch of living materials when the proportions of infected areas reach 80%. Among them, the total population of Taoyuanju and Meihua Villa are large, and the limited supplies in the vicinity cannot fully meet their living needs under the epidemic. However, such neighborhoods as Zhenye City, St. Morris, and Ling Scare New Village are small in size but far from supermarkets, and cannot be immediately resupplied when there is a shortage of living materials. In addition, there are also several neighborhoods such as Aegean Sea and Telford Garden, although they are located in areas with developed transportation and several large supermarket chains nearby, they are more populated and densely distributed, creating some competition for the limited living materials, thus leading to a shortage of supply in some places relatively far away from the supermarkets.

4.2.4 Spatial distribution pattern of mismatch degree between supply and demand of residents' living materials

1) global spatial autocorrelation

Through the spatial autocorrelation analysis of the mismatch degree of material supply and demand, it is found that the P values are all less than the significant level of 0.01 At the same time, the Moran's I index is greater than 0.5 and the Z score is far greater than 2.58, indicating that the spatial distribution of the mismatch degree of living material supply and demand shows a significant agglomeration effect.

The number of infections at the initial stage of virus transmission was small. Confirmed cases in the simulated situation were more spatially dispersed. Hence, the characteristics of spatial clustering were not obvious. As the number of infected people increased, more and more cases appeared in residential buildings, which led to the related buildings being closed and managed. People's access to daily life materials was restricted, and material mismatch phenomenon appeared in these areas. The spread of the virus was more serious in crowded places, thus leading to the degree of material mismatch appearing more strongly in spatial agglomeration.

Index	Moran's I	Z-value	P-value
δ（20%）	0.692	26.381	0.00
δ（40%）	0.748	27.787	0.00
δ（60%）	0.743	27.334	0.00
δ（80%）	0.769	27.991	0.00

Table 5. Moran's I value of mismatch degree of material supply and demand under different simulation degrees

2) local spatial autocorrelation

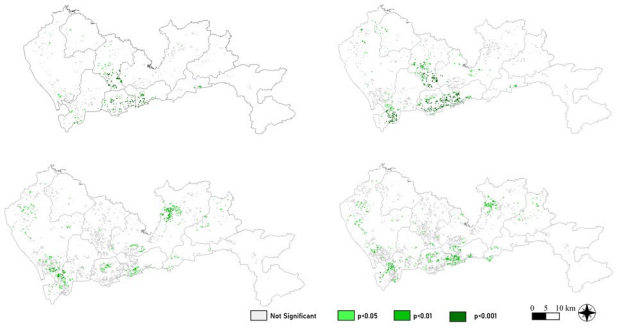

Figure 9. Lisa cluster of mismatch degree of living materials

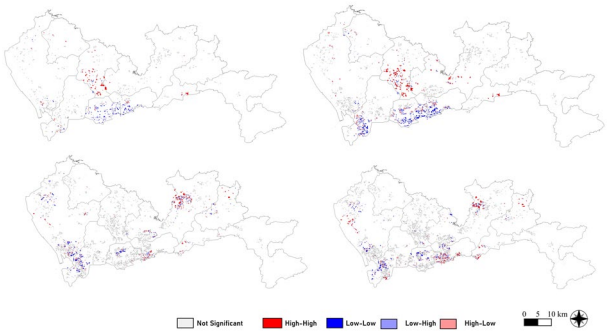

Figure 10. Lisa significance of mismatch degree of living materials

Lisa clustering map and significance map are used to study the instability of local space. Generally speaking, the local space of the mismatch degree of residents' living materials is mainly characterized by "low-low" agglomeration and "high-high" agglomeration. The agglomeration effect becomes more and more significant with the development of the epidemic spreading. Low-low clusters are mainly in Futian District, Luohu District and the south of Nanshan District. These areas have good material support and convenient transportation, which is convenient for residents to obtain materials. High-high clusters are mainly in the south of Longhua District and the north of Longgang District. These regions have a large population and a large demand for materials, but the material supply is

insufficient. They are cluster areas with weak material supply, which need to be paid special attention to.

5. CONCLUSIONS

The outbreak of COVID-19 has seriously threatened people's lives and health. The guarantee of living materials is related to the basic life of hundreds of millions of people and is of great significance to the effective and orderly prevention and control of the epidemic. Through the integration of infectious disease model and spatial analysis, this paper studies the mismatch of supply and demand of living materials according to different epidemic simulation situations. From the perspective of the whole city, the residential buildings with unbalanced supply and demand are mostly distributed in the southwest of Bao'an District, the southern of Longhua District and Longgang District. Such as Plum Blossom Villa and St. Morris in Longhua District, Taoyuan Residence and Qunle Building in Bao'an District. In terms of the spatial agglomeration of spatial mismatch degree, generally speaking, the local space of the mismatch degree of residents' living materials in Shenzhen is mainly manifested in low-low agglomeration and high-high agglomeration. Low low clusters are mainly Futian District, Luohu District and the south of Nanshan District. High high clusters are mainly in the south of Longhua District and the north of Longgang District. The results provide useful insights into the optimization and adjustment of the spatial layout of living materials supplier under the fine epidemic prevention and control in Shenzhen.

ACKNOWLEDGEMENTS

The study is jointly supported by the National Key Research and Development Project (2019YFB2103104), Natural Science Foundation Project of China (42071360), and The Tencent-WeChat Tencent Rhino-bird Project (JR-WXG-2021131).

REFERENCES

Ala ' raj, M., Majdalawieh, M., & Nizamuddin, N. (2021). Modeling and forecasting of COVID-19 using a hybrid dynamic model based on SEIRD with ARIMA corrections. *Infectious Disease Modelling*, 6, 98-111.

Annas, S., Pratama, M. I., Rifandi, M., Sanusi, W., & Side, S. (2020). Stability analysis and numerical simulation of SEIR model for pandemic COVID-19 spread in Indonesia. *Chaos, Solitons & Fractals*, 139, 110072.

Apparicio, P., Cloutier, M. S., & Shearmur, R. (2007). The case of Montreal's missing food deserts: evaluation of accessibility to food supermarkets. *International Journal of Health Geographics*, 6(1), 1-13.

Cavalcante, A. L. B., de Faria Borges, L. P., da Costa Lemos, M. A., de Farias, M. M., & Carvalho, H. S. (2021). Modelling the spread of covid-19 in the capital of Brazil using numerical solution and cellular automata. *Computational Biology and Chemistry*, 94, 107554.

Charreire, H., Casey, R., Salze, P., Simon, C., Chaix, B., Banos, A., & Oppert, J. M. (2010). Measuring the food environment using geographical information systems: a methodological review. *Public Cealth Cutrition*, 13(11), 1773-1785.

Firozjaei, M. K. , Fathololomi, S. , Kiavarz, M., Arsanjani, J. J., & Alavipanah, S. K. (2021). Modeling the impact of the covid-19 lockdowns on urban surface ecological status: a case study of milan and wuhan cities. *Journal of Environmental Management*, 112236.

Götz, T., & Heidrich, P. (2020). Early stage COVID-19 disease dynamics in Germany: models and parameter identification. *Journal of Mathematics in Industry*, 10(1), 1-13.

Kermack, W. O. (1927). A contribution to the mathematical theory of epidemics. *Proceedings of Royal Society Series A*, 115.

Lahrouz, A., & Omari, L. (2013). Extinction and stationary distribution of a stochastic sirs epidemic model with non-linear incidence. *Statistics & Probability Letters*, 83(4), 960-968.

Leclair, M. S., & Aksan, A. M. (2014). Redefining the food desert: combining gis with direct observation to measure food access. *Agriculture & Human Values*, 31(4), 537-547.

Ma, J. , Hua, T., Zeng, K., Zhong, B., & X Liu. (2020). Influence of social isolation caused by coronavirus disease 2019 (covid-19) on the psychological characteristics of hospitalized schizophrenia patients: a case-control study. *Translational Psychiatry*, 10(1).

Schimit, P. H. (2021). A model based on cellular automata to estimate the social isolation impact on COVID-19 spreading in Brazil. *Computer Methods and Programs in Biomedicine*, 200, 105832.

Tu W., Cao J., Gao Q., Cao R., Fang Z., Yue Y., LI Q. Sensing Urban Dynamics by Fusing Multi-sourced Spatiotemporal Big Data. *Geomatics and Information Science of Wuhan University*, 2020, 45(12): 1875-1883. doi: 10.13203/j.whugis 20200535

White, S. H., Del Rey, A. M., & Sánchez, G. R. (2007). Modeling epidemics using cellular automata. *Applied Mathematics and Computation*, 186(1), 193-202.

Yang, Z., Zeng, Z. , Wang, K. , SS Wong, & He, J. (2020). Modified seir and ai prediction of the epidemics trend of covid-19 in china under public health interventions. *Journal of Thoracic Disease*, 12(3), 165-174.

Zhao, T., Tu, W., Fang, Z., Wang, X., Huang, Z., Xiong, S., & Zheng, M. (2021). Optimizing living material delivery during the COVID-19 Outbreak. *IEEE Transactions on Intelligent Transportation Systems,* 1-11.